ORIGINAL ARTICLE

Equilibrium melting temperature and crystallization kinetics of α- and β′-PBN crystal forms

Michelina Soccio, Nadia Lotti, Lara Finelli and Andrea Munari

The melting behavior and crystallization kinetics of PBN–PDEN and PBN–PTDEN copolymers were investigated using differential scanning calorimetry. Multiple endotherms were observed in all of the copolymers under investigation, originating from melting and recrystallization processes. By applying the Hoffman–Weeks method, the T_m° of the α and β′-PBN phases were derived. The T_m° value of the β′-form, which has not been determined before, is significantly higher, as expected, because the β′-phase is thermodynamically favored and more tightly packed. The isothermal crystallization kinetics were analyzed according to the Avrami treatment. The presence of either oxygen or sulfur atoms in the PBN polymeric chain was found to reduce its crystallizability. In particular, the crystallization rate regularly decreased as the co-unit content was increased. Lastly, the α-PBN phase was found to crystallize faster than β′-one, which is expected, as it the more kinetically favored phase.
Polymer Journal (2012) **44**, 174–180; doi:10.1038/pj.2011.112; published online 9 November 2011

INTRODUCTION

Naphthalene-containing thermoplastic polyesters have attracted an increasing degree of interest in recent years. Poly(ethylene naphthalate), poly(butylene naphthalate) and poly(propylene naphthalate) are the best known members of this family of thermoplastics. These newly developed high-performance polymers that contain a rigid naphthalene ring and a flexible alkylene group in the repeat unit exhibit physical and mechanical properties superior to the widely used corresponding phthalate-based polyesters. In particular, poly(butylene 2,6-naphthalate) (PBN) is characterized by very good gas barrier properties, high UV resistance, high solvent-resistance, long-term electrical properties and thermostability. To date, two crystalline structures for PBN, denoted as α- and β-forms, have been acknowledged. The transition between these two forms can take place reversibly by mechanical deformation.[1] Ju *et al.* investigated the crystalline forms of PBN samples obtained by different thermal treatments in bulk. The α-form was produced by annealing a quenched sample in the solid state or by crystallizing PBN from the static melt at temperatures lower than 225 °C. An exclusive β′-form was generated by performing non-isothermal crystallization from the melt at an extremely low cooling rate (0.1 °C per min). This thermally prepared β′-form is characterized by a WAXD profile similar to that of the β-form obtained by mechanical deformation, except for the substantial *d*-spacing deviation in the (0–11) and (010) planes.[2] Nevertheless, if PBN is melt crystallized at high T_c, both the α and β′-forms are obtained simultaneously, and their relative ratio is dependent on the adopted crystallization temperature. Additionally, changes in the crystalline form never occur in the solid state. Lastly,

the main difference between the α and β′ crystal structures lies in the packing efficiency of the crystal chains, the β′-form being more tightly packed.[2] Recently, we demonstrated that the pure β′-form can also be obtained by the copolymerization of PBN with both poly(diethylene naphthalate) (PDEN) and poly(thiodiethylene naphthalate) (PTDEN).[3,4] The most relevant result of these studies concerned the crucial importance of copolymer composition in determining the selective formation of one form. In particular, the α-form was always detected in copolymers containing a low amount of comonomeric units (20 mol % in the case of DEN, 10 mol % in the case of TDEN), and the β′-crystal phase developed in copolymers containing 40 mol % DEN units or 30 and 40 mol % TDEN units, independently of the thermal treatment. In the case of PBN–PDEN30 and PBN–PTDEN20, an effect of the thermal treatment has been observed: the α- or β′-form was obtained at a low or high cooling rate, respectively. Taking into account the fact that the β′-form is more thermodynamically stable and more tightly packed, its selective formation in the copolymers with the highest content of co-units has been ascribed to the higher mobility and flexibility of the polymeric chains because of the presence of a significant amount of either oxygen or sulfur atoms. Lastly, a comparison between the two copolymeric systems indicated that the formation of the β′-form was favored in PBN–PTDEN copolymers, probably because of the higher packing efficiency. This result was ascribed to the larger dimensions of the sulfur atoms, which are very similar to those of neighboring methylene groups, and to the higher chain flexibility due to the longer C–S–C bonds. These prior results showed that it would be interesting to investigate the effect of the copolymer composition on the crystallization rate of PBN samples isothermally crystallized from the melt,

Dipartimento di Ingegneria Civile, Ambientale e dei Materiali, Università di Bologna, Bologna, Italy
Correspondence: Professor N Lotti, Dipartimento di Ingegneria Civile, University of Bologna, Via Terracini 28, Bologna 40131, Italy.
E-mail: nadia.lotti@mail.ing.unibo.it

because the α and β′ phases are selectively formed depending on the co-unit content. To the best of our knowledge, the literature does not report data of the equilibrium melting temperature of the β′-phase. Therefore, a further aim of this work is to determine T_{m}° of β′ and compare it with the value of the α phase.

EXPERIMENTAL PROCEDURE
Materials
Poly(butylene/diethylene naphthalate) (PBN–PDEN) and poly(butylene/thio-diethylene naphthalate) copolymers (PBN–PTDEN) were synthesized according to the well-known two-stage polycondensation procedure, as previously reported,[3,4] starting from different ratios of 1,4-butanediol/diethylene glycol or 1,4-butanediol/thiodiethylene glycol, and from dimethyl naphthalate, employing titanium tetrabutoxide as catalyst. The two copolymeric systems can be represented as follows:

PBN–PDEN

PBN–PTDEN
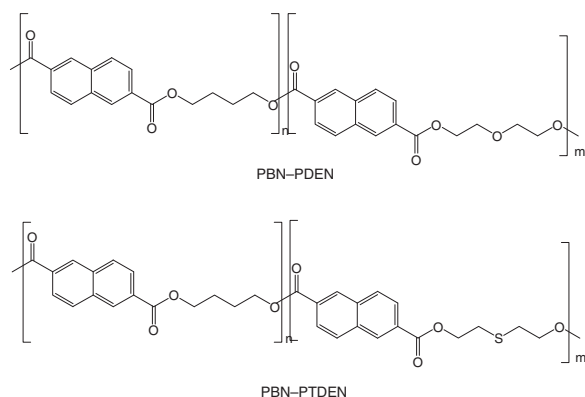
We previously characterized the molecular and thermal properties of these copolymers.[3,4] The chemical structure was confirmed by ^{1}H-NMR, and the number molecular weights were determined by gel permeation chromatography (GPC). The molecular and thermal characterization data are reported in Table 1.

Calorimetric measurements
The isothermal crystallization behaviors of PBN–PDEN and PBN–PTDEN copolymers were investigated with a Perkin–Elmer DSC7 calorimeter. The external block temperature control was set at −60 °C. All measurements were carried out under a nitrogen atmosphere to minimize oxidative degradation. The instrument was calibrated with high-purity standards (indium and cyclohexane) for melting temperature and heat of fusion. Heating rates of 10, 20, 30 and 40 °C/min were used whenever needed. Relatively small samples (∼5 mg) were used to minimize the thermal conductivity of the polymer; a fresh specimen was used for each run.

To erase the previous thermal history, the samples were heated to ∼40 °C above fusion temperature at a rate of 20 °C per min, held there for 3 min, and

then rapidly cooled by liquid nitrogen to the predetermined crystallization temperature T_{c}. The T_{c} range was chosen to avoid crystallization on the cooling step and to obtain crystallization times no longer than 60 min. The evolution of the heat flow during the isothermal crystallization was recorded as a function of time, and the completion of the crystallization process was detected by the leveling of the differential scanning calorimetry (DSC) trace. For a better definition of the starting time (t_{start}), a blank run was also performed for each isothermal scan, with the same sample at a temperature above the maximum of the melting endotherm at which no phase change occurred.[5] The blank run was subtracted from the isothermal crystallization scan, and the start of the process was taken as the intersection of the extrapolated baseline and the resulting exothermal curve. The isothermally crystallized samples were then heated directly from T_{c} to melting at 10 °C per min. The melting temperature (T_{m}) was taken as the peak value of the endothermic phenomenon of the DSC curve.

RESULTS AND DISCUSSION
Melting behavior
Before analyzing the melting behavior of the copolymers under investigation, it is worth mentioning that after melt quenching, the selective formation of the α- or β′-phases occurred, depending on composition. The results previously obtained[3,4] are summarized in Table 2.

Figure 1 shows typical calorimetric traces of PBN–PDEN10, PBN–PDEN40, PBN–PTDEN10 and PBN–PTDEN40, isothermally crystallized at various temperatures (T_{c}) according to the thermal treatment described in the Experimental Procedure section.

As can be seen, multiple endotherms appear in the thermograms on heating, the peaks of which have been labeled with Roman numerals (I to III) in order of increasing temperature. The dependence of the position and intensity of the endotherms on temperature can be observed. In particular, the temperature of endotherm I is ∼5 °C above T_{c}; the position of melting peak II shifts to higher temperature

Table 2 Crystal phase obtained after melt quenching and equilibrium melting temperature ($T_{\mathrm{m,co}}^{\circ}$)

Samples	Crystal phase[a]	$T_{m,co}^{\circ}$ (°C)
PBN–PDEN10	α	246
PBN–PDEN20	α	231
PBN–PDEN30	β′	236
PBN–PDEN40	β′	220
PBN–PTDEN10	α	242
PBN–PTDEN20	β′	246
PBN–PTDEN30	β′	227
PBN–PTDEN40	β′	217

[a]From refs 3,4.

Table 1 Molecular and thermal characterization data

| Copolymer | Co-unit content (mol %) | | M_n | First | | Second | | | | | |
	(feed)	(^{1}H-NMR)		T_m (°C)	ΔH_m (J/g)	T_g (°C)	Δc_p (J/g°C)	T_c (°C)	ΔH_c (J/g)	T_m (°C)	ΔH_m (J/g)
PBN–PDEN10	10	7	27 000	233	44	75	0.114	106	8	232	47
PBN–PDEN20	20	14	25 100	223	39	71	0.131	102	15	223	40
PBN–PDEN30	30	23	30 440	212	35	68	0.148	80	35	211	35
PBN–PDEN40	40	33	28 200	194	31	65	0.17	81/103	29	193	30
PBN–PTDEN10	10	9.5	36 400	229	72	72	0.068	83	14	227	58
PBN–PTDEN20	20	16.5	30 500	221	66	66	0.038	80	39	219	41
PBN–PTDEN30	30	30	31 000	200	61	61	0.073	75/88	37	199	38
PBN–PTDEN40	40	35	31 400	191	58	58	0.087	73/94	32	189	32
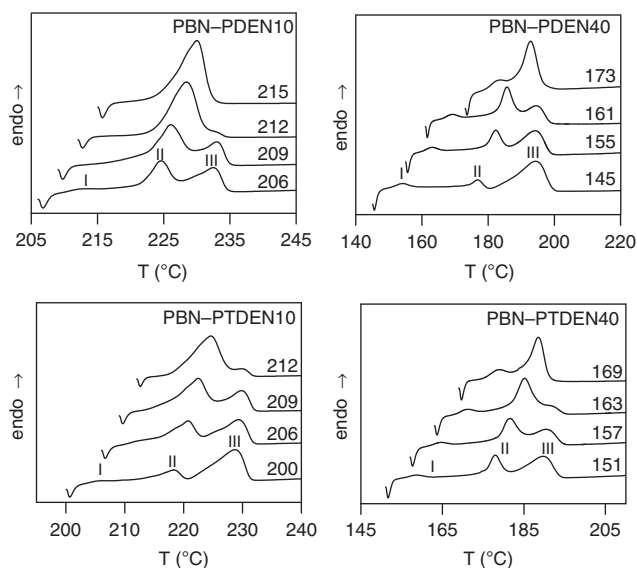
Figure 1 DSC melting endotherms after isothermal crystallization at the indicated values of T_c (heating rate: 10 °C per min).
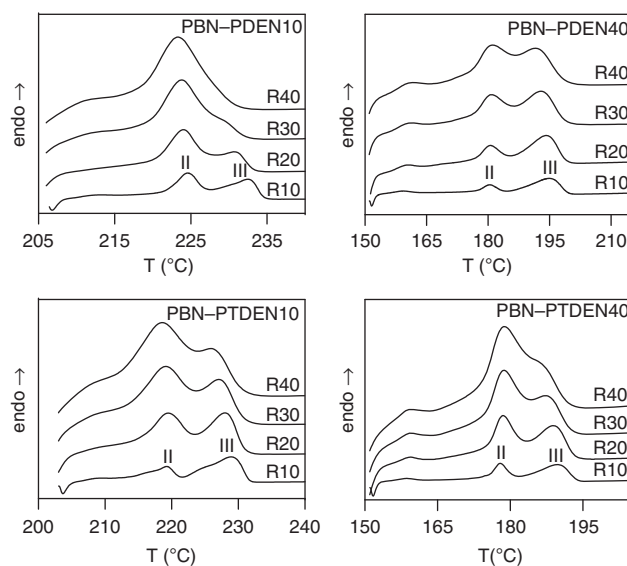

Figure 2 DSC melting endotherms of PBN–PDEN10, PBN–PDEN40, PBN–PTDEN10 and PBN–PTDEN40 scanned at the indicated heating rates (°C per min) after isothermal crystallization at 206 °C, 151 °C, 203 °C and 151 °C, respectively. The curves have not been corrected for changes in the instrumental signal with heating rate.

and its magnitude increases as the crystallization temperature increases. The position of endotherm III remains unchanged, while its magnitude decreases with increasing T_c. In general, there are two main reasons for the appearance of multiple melting endotherms. More than one DSC endothermic peak can result from the melting of different crystal types within the sample if each is present before thermal treatment.[6–8] Multiple endothermic peaks can also be caused by the partial melting of some or all of the original material and its reorganization into material of higher order during the thermal analysis, before the final melting.[9,10] The observed dependence of the multiple endotherms on the crystallization temperature permits to hypothesize the origin of each peak. In particular, peak I can be considered a typical 'annealing peak' that can be associated with the melting of poorer crystals that grow between the larger crystals at T_c. Endotherm II can be ascribed to the fusion of crystals grown by normal primary crystallization during the isothermal period at T_c; its dependence on the crystallization temperature, in terms of both peak position and area, suggests that thicker crystalline lamellae develop with increasing T_c. The high temperature, melting peak (III) can be explained as the result of the melting of crystals with higher stability and perfection, grown during the heating run as a consequence of recrystallization or reorganization of crystals initially formed during the isothermal crystallization. To confirm the possibility of melting–recrystallization processes in the samples under investigation, the effect of the heating rate on the melting behavior was evaluated. As shown in Figure 2, the magnitude of melting peak II increased as the heating rate was increased, in contrast to the high–temperature melting peak III, the magnitude of which regularly decreased with the heating rate. The higher value of the heat of fusion of melting peak II at the faster heating rate indicates that the crystals formed at T_c do not have enough time to melt and recrystallize, confirming the role of a mechanism based on melting and recrystallization of less perfect crystallites into thicker crystals that melt at higher temperature.

The phenomenon of multiple melting endotherms observed in PBN has already been the subject of intense studies and has been ascribed to melting and recrystallization processes taking place during the DSC scan.[11–14]

To compare the crystallization rates of the samples under investigation, the measurement of the equilibrium melting temperature (T_m°) is of great importance, because it is needed to determine the dependence of the rate of crystallization on the degree of undercooling, $\Delta T = T_m^\circ - T_c$. One of the most commonly used procedures to determine T_m° is the Hoffman–Weeks method.[15] The popularity of this approach is a result of its simplicity, as only the experimental melting temperature of the crystallites formed at T_c is required. Nevertheless, Marand and co-workers[16,17] recently discussed the validity of the basic premise of the linear Hoffmann–Weeks treatment: that is, the thickening coefficient for lamellae, γ, taken as independent of T_c and time.[18–20] As demonstrated by some results in the literature,[16–21] the linear extrapolation, when carried out for lamellar crystals exhibiting a constant γ value, invariably underestimates T_m° and leads to an overestimation of the γ value. In fact, the Hoffmann–Weeks procedure does not account for the significant contribution to the difference between the melting and crystallization temperatures that arises from the temperature dependence of the fold surface free energy and the thickness increment above the minimum (thermodynamic) lamellar thickness. Neglecting this contribution causes an underestimation of the equilibrium melting temperature and an overestimation of the thickening coefficient. Moreover, for copolymers, the concept of infinite lamellar thickness is not appropriate, even though this treatment is frequently applied to these systems to calculate the driving force for crystallization (namely the degree of undercooling $\Delta T = T_m^\circ - T_c$). Notwithstanding the above limitations, the experimental melting temperatures (T_m) of PBN–PDEN and PBN–PTDEN copolymers crystallized at different T_cs were used to obtain information on the equilibrium melting temperature ($T_{m,co}^\circ$) by means of the Hoffman–Weeks' relationship:[15]

$$T_m = T_m^\circ(1 - 1/\gamma) + T_c/\gamma \qquad (1)$$

where γ is a factor that depends on the lamellar thickness. More precisely, $\gamma = l/l^\star$, where l and $l^\star$ are the thickness of the grown

Figure 3 Peak temperatures of the (●) II and (■) III endotherms as a function of T_c and linear extrapolation according to the Hoffman–Weeks treatment for copolymers crystallizing in the α-form.
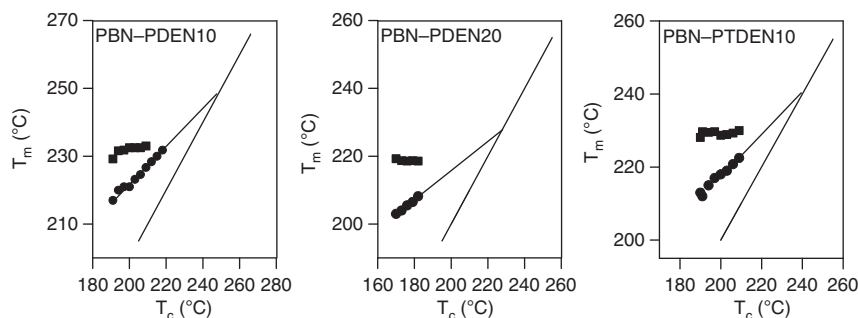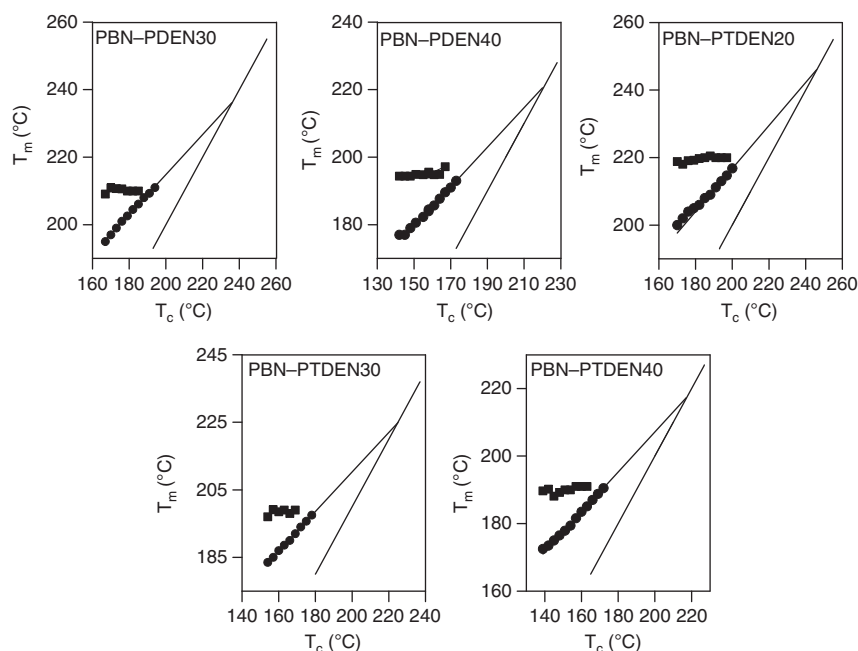

Figure 4 Peak temperatures of the (●) II and (■) III endotherms as a function of T_c and linear extrapolation according to the Hoffman–Weeks treatment for copolymers crystallizing in the β′-form.

crystallite and of the critical crystalline nucleus, respectively. Note that Equation (1) correctly represents the experimental data only when γ is constant and the slope of the curve in a plot of T_m versus T_c is approximately equal to 0.5.

The peak values of endotherms II and III as a function of T_c are plotted in Figures 3 and 4 for all of the polymers under investigation.

Endotherm II is clearly related to the original main crystal population, and its location reflects the higher perfection of the crystals grown at higher temperatures. Melting endotherm III is observed at a relatively constant temperature, which is characteristic of material that is partially recrystallized into a more stable form on heating. With the increment of T_c, the perfection of the originally grown crystals increases up to a point at which no further recrystallization can occur during the DSC run, and endotherm III disappears. In Figures 3 and 4, the linear extrapolations of the experimental data up to the $T_m=T_c$ lines are also drawn, and the $T_{m,co}^\circ$ values

obtained are collected in Table 2. These values are plotted as a function of the butylene naphthalate unit content in Figure 5 (left panels) for the α- and β′-phases, and $T_{m,co}^\circ$ decreases with the increasing co-unit content.

Melting point depression can be caused by a reduction in the thickness of lamellar crystals as well as an increase in the level of crystal imperfection.

Several theories have been developed to explain copolymer crystallization and are commonly classified into two categories: the comonomer exclusion[22,23] and comonomer inclusion models.[24,25] In particular, when only one co-unit can crystallize and the second one is completely excluded from the crystals (as in the case of the copolymers under investigation), melting point reduction is usually examined using Flory's equation. Flory's treatment,[22] commonly used in the past and derived under the assumption that fusion concerns the disappearance of long sequences of crystallizable units, underestimates the melting point depression of random copolymers. The concentra-
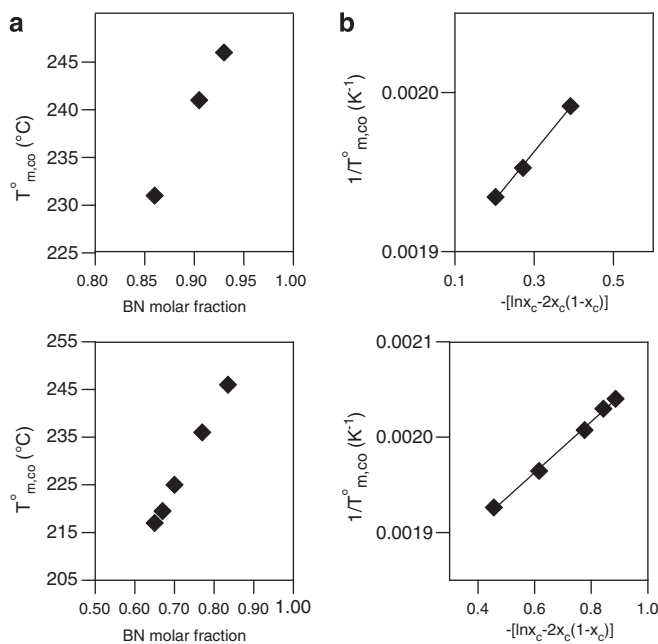
178

Figure 5 (a) Equilibrium melting temperatures ($T_{m,co}^{\circ}$) as a function of composition; (b) $1/T_{m,co}^{\circ}$-composition plots according to Baur's equation. Data for copolymers crystallizing in the α- and β′-forms are shown on the top and bottom, respectively.

tion of long sequences actually decreases with increasing co-unit content, and the experimental T_m values are consequently lower than those postulated by the theory. The equation proposed by Baur[23] takes into account the effect of the sequence length of crystallizable units that can crystallize only when their length corresponds to the crystal thickness. Baur's equation is given by:[23]

$$1/T_{m,co}^{\circ} = 1/T_m^{\circ} - (R/\Delta H_m^{\circ})(\ln x_C - 2x_C(1 - x_C)) \quad (2)$$

where $T_{m,co}^{\circ}$ is the melting temperature of a random copolymer with mole fraction x_C of crystallizable comonomer C, T_m° is the equilibrium melting temperature of the homopolymer (in this case PBN) and R is the gas constant. On the basis of equation (2), the $T_{m,co}^{\circ}$ values were reciprocally plotted against $-[\ln x_C - 2x_C(1 - x_C)]$ in Figure 5 (right panels), and the equilibrium melting temperature and heat of fusion for the completely crystalline α-PBN or β′-PBN were extrapolated. The plot shows good linearity, and this result can be considered to be further proof of the random nature of the copolymers investigated, as well as evidence of the exclusion of the co-units from the crystalline lattice of PBN. The estimated T_m° values were found to be 261 and 281 °C for the α- and β′-phases, respectively. The value of the α-phase is in excellent agreement with the value found in our previous work.[26] The datum corresponding to the β′ phase, to our knowledge, is the first such value reported in the literature. However, it has to be pointed out that $T_{m,\alpha\text{-phase}}^{\circ}$ is significantly lower than $T_{m,\beta'\text{-phase}}^{\circ}$. This result is not surprising when it is considered that the β′-phase is thermodynamically favored and more tightly packed than the α-phase.

Isothermal crystallization kinetics

The analysis of the isothermal crystallization kinetics can be carried out according to the well-known Avrami equation:[27]

$$X_t = 1 - \exp[-k_n(t - t_{start})^n] \quad (3)$$

where X_t is the fraction of polymer crystallized at time t; k_n is the overall kinetic constant; t is the time of the isothermal step measured from the achievement of temperature control; t_{start} is the initial time of the crystallization process, as described in the experimental section; and n is the Avrami exponent, which is dependent on the nucleation mechanism and the morphology of the growing crystallites. X_t can be calculated as the ratio between the area of the exothermic peak at time t and the total measured area of crystallization. The value of the kinetic constant k_n is typically obtained from the following relationship:

$$k_n = \ln 2/t_{1/2}^n \quad (4)$$

where $t_{1/2}$ is the crystallization half-time, defined as the time required to reach $X_t = 0.5$.

Equation 3 is usually applied to the linearized form of the experimental data by plotting $[\ln(-\ln(1-X_t)]$ as a function of $\ln(t - t_{start})$, permitting the determination of n and k_n from the slope and the intercept, respectively.

The crystallization half-time $t_{1/2}$, the parameter n, and the kinetic constants k_n are collected in Table 3. For all samples under investigation, the overall kinetic constant k_n regularly decreases with increasing T_c as usual at low undercooling, where the crystal formation is controlled by nucleation. For the isothermally crystallized PBN–PDEN and PBN–PTDEN samples, the Avrami exponent n was close to 3 at all of the crystallization temperatures investigated (see Table 3), indicating that the crystallization process originates from predetermined nuclei and is characterized by a three-dimensional spherulitic growth.

To evaluate the effect of composition on the crystallization rate of PBN, the half-crystallization time $t_{1/2}$ was plotted as a function of ΔT in Figure 6, along with the data concerning the homopolymer PBN.[26]

The value of $t_{1/2}$ regularly increases as the co-unit content is increased, independently of the chemical structure of the comonomeric unit (DEN or TDEN, see Figure 6). Because the crystallization process in these copolymers involves the segregation of the co-units, the observed decrease of the crystallization rate with the increasing co-unit content can be considered to be due to the rejection from the crystalline phase of these units, which makes the regular packing of the PBN polymer chains more difficult. In the results reported in Figure 6, two distinct groups of data can be observed, each of which is related to one of the two crystalline phases of PBN.

Considering PBN–PDEN20 and PBN–PTDEN20, which are characterized by very similar copolymer composition but crystallize in the α and β′-form, respectively, it is evident that the α-phase crystallizes much faster than β′-phase. This result is in agreement with the data reported in the literature that indicates that the α-PBN form is kinetically favored.

CONCLUSIONS

The random incorporation of diethylene naphthalate or thiodiethylene naphthalate comonomeric units along the polymeric chain of PBN resulted in new materials that are able to selectively develop into the α- or β′-crystal phase, simply by changing the copolymer composition. The investigation of the crystallization kinetics and melting behavior of these new copolymeric systems permitted the determination of the following:

(i) the equilibrium melting temperatures of both phases, in particular, $T_{m,\alpha\text{-form}}^{\circ}$ was found to be lower than $T_{m,\beta'\text{-form}}^{\circ}$, as expected because the β′-phase is more tightly packed.

(ii) the crystallization rate of both phases, and the fact that the α-phase crystallizes significantly faster than the β′-phase.

Table 3 Kinetic parameters for the isothermal crystallization of PBN–PDEN and PBN–PTDEN copolymers

Sample	T_c (°C)	$t_{1/2}$ (min)	n	k_n (s^{-n})
PBN–PDEN10	191	0.8	2.6	3.3×10^{-4}
	194	1.3	2.7	2.5×10^{-5}
	197	2.1	2.8	2.1×10^{-7}
	200	3.5	3.0	4.0×10^{-8}
	203	5.0	3.0	2.9×10^{-8}
	206	7.4	2.9	8.6×10^{-9}
	209	10.0	3.0	2.2×10^{-9}
	212	14.5	3.0	1.4×10^{-9}
PBN–PDEN20	173	0.7	2.6	9.8×10^{-5}
	176	1.5	2.7	6.5×10^{-7}
	179	2.1	2.6	3.1×10^{-7}
	182	3.3	2.8	8.1×10^{-8}
	185	5.5	3.0	3.4×10^{-8}
	188	8.4	3.1	2.4×10^{-9}
	191	11.8	3.0	1.5×10^{-9}
PBN–PDEN30	167	1.6	2.7	1.7×10^{-5}
	170	1.7	2.8	3.1×10^{-7}
	173	2.2	2.7	1.4×10^{-7}
	176	2.9	2.8	1.9×10^{-7}
	179	4.1	2.9	2.7×10^{-8}
	182	6.2	2.8	1.0×10^{-8}
	185	9.7	3.1	3.9×10^{-9}
	188	14.4	2.9	1.5×10^{-9}
PBN–PDEN40	145	2.5	2.6	4.9×10^{-6}
	148	3.1	2.6	6.0×10^{-8}
	151	3.3	2.7	4.3×10^{-8}
	155	4.2	2.7	4.0×10^{-8}
	158	4.6	2.8	3.2×10^{-8}
	161	5.9	2.7	1.3×10^{-8}
	164	6.3	2.9	1.0×10^{-8}
	167	8.4	2.8	7.4×10^{-9}
	170	13.3	3.0	3.4×10^{-9}
PBN–PTDEN10	191	2.0	2.6	2.8×10^{-5}
	194	3.3	2.7	1.1×10^{-6}
	197	5.5	3.1	4.1×10^{-8}
	200	7.5	3.0	2.9×10^{-9}
	203	11.0	2.9	2.1×10^{-9}
	206	15.1	2.8	9.0×10^{-10}
	209	19.9	3.0	3.1×10^{-10}
PBN–PTDEN20	170	0.8	2.7	2.0×10^{-4}
	173	0.9	2.7	3.9×10^{-5}
	176	1.0	2.8	2.0×10^{-6}
	179	1.1	2.9	1.3×10^{-6}
	182	1.2	2.8	1.1×10^{-6}
	185	1.6	3.0	8.8×10^{-7}
	188	2.0	3.0	5.0×10^{-7}
	191	3.5	2.9	6.5×10^{-8}
	194	5.7	3.0	1.9×10^{-8}
	197	11.3	2.8	2.0×10^{-9}
PBN–PTDEN30	154	1.7	2.6	5.7×10^{-5}
	157	1.8	2.6	9.8×10^{-6}
	160	2.1	2.7	2.7×10^{-7}
	163	2.9	2.8	7.1×10^{-8}

Table 3 (Continued)

Sample	T_c (°C)	$t_{1/2}$ (min)	n	k_n (s^{-n})
	166	3.9	2.7	4.4×10^{-8}
	169	5.5	2.9	1.6×10^{-8}
	172	8.7	3.0	6.9×10^{-9}
	175	14.1	3.0	2.1×10^{-9}
	178	17.7	2.9	5.9×10^{-10}
PBN–PTDEN40	139	2.2	2.7	4.4×10^{-5}
	142	2.3	2.8	5.0×10^{-6}
	145	3.0	2.7	8.1×10^{-8}
	148	3.2	2.8	5.6×10^{-8}
	151	3.4	2.8	8.0×10^{-8}
	154	3.7	2.9	5.9×10^{-8}
	157	4.7	2.7	3.0×10^{-8}
	160	6.2	2.8	1.9×10^{-8}
	163	7.7	2.9	7.6×10^{-9}
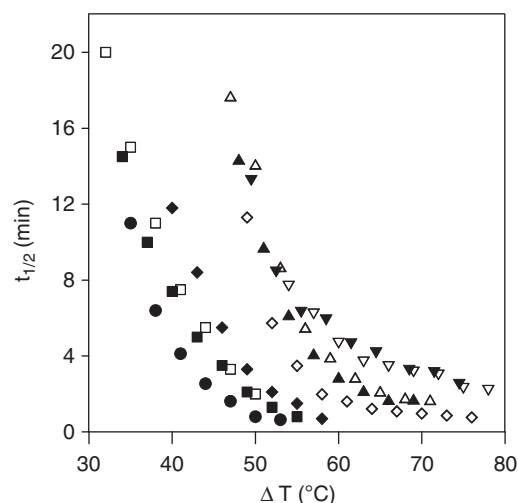
Figure 6 Crystallization half-time ($t_{1/2}$) vs undercooling degree ($\Delta T = T_m^{\circ} - T_c$) for: (●) PBN (from ref. 17); (■) PBN–PDEN10; (♦) PBN–PDEN20; (▲) PBN–PDEN30; (▼) PBN–PDEN40; (□) PBN–PTDEN10; (◇) PBN–PTDEN20; (△) PBN–PTDEN30; (▽) PBN–PTDEN40.

1 Watanabe, H. Stretching and structure of polybutylene-naphthalene-2, 6-dicarboxylate films. *Kobunshi. Ronbunshu.* **33,** 229–237 (1976).
2 Ju, M. Y., Huang, J. M. & Chang, F. C. Crystal polymorphism of poly(butylene-2,6-naphthalate) prepared by thermal treatments. *Polymer* **43,** 2065–2074 (2002).
3 Soccio, M., Gazzano, M., Lotti, N., Finelli, L. & Munari, A. Copolymerization: a new tool to selectively induce poly(butylene naphthalate) crystal form. *Polymer* **51,** 192–200 (2010).
4 Soccio, M., Gazzano, M., Lotti, N., Finelli, L. & Munari, A. Synthesis and characterization of novel random copolymers based on PBN: influence of thiodiethylene naphthalate co-units on its polymorphic behaviour. *Polymer* **51,** 192–200 (2010).
5 Righetti, M. C. & Munari, A. Influence of branching on melting behavior and isothermal crystallization of poly(butylene terephthalate). *Macromol. Chem. Phys.* **198,** 363–378 (1997).
6 Marand, H., Alizadeh, A., Farmer, R., Desai, R. & Velikov, V. Influence of structural and topological constraints on the crystallization and melting behavior of polymers. 2. Poly(arylene ether ether ketone). *Macromolecules* **33,** 3392–3403 (2000).
7 Chung, J. S. & Cebe, P. Melting behavior of poly(phenylene sulfide). 2. Multiple-stage melt crystallization. *Polymer* **33,** 2312–2324 (1992).
8 Lemstra, P. J., Schouten, A. J. & Challa, G. Secondary crystallization of isotatic polystyrene. *J. Polym. Sci. Polym. Phys. Ed.* **12,** 1565–1574 (1974).

9 Minakov, A. A., Mordvinsted, D. A. & Schick, C. Melting and reorganization of poly (ethylene terephthalate) on fast heating (1000 K/s). *Polymer* **45,** 3755–3763 (2004).

10 Kong, Y. & Hay, J. N. Multiple melting behaviour of poly(ethylene terephthalate). *Polymer* **44,** 623–633 (2002).

11 Yasuniwa, M., Tsubakihara, S., Fujioka, T. & Dan, Y. X-ray studies of multiple melting behavior of poly(butylene-2,6-naphthalate). *Polymer* **46,** 8306–8312 (2005).

12 Papageorgiou, G. & Karayannidis, G. Multiple melting behaviour of poly(ethylene-co-butylene naphthalate-2,6-dicarboxylate)s. *Polymer* **40,** 5325–5332 1999.

13 Ju, M. & Chang, F. C. Multiple melting behavior of poly(butylene-2,6-naphthalate). *Polymer* **42,** 5037–5045 (2001).

14 Yasuniwa, M., Tsubakihara, S. & Fujioka, T. X-ray and DSC studies on the melt-recrystallization process of poly(butylenes naphthalate). *Thermochim. Acta.* **396,** 75–78 (2003).

15 Hoffman, J. D. & Weeks, J. J. Melting process and equilibrium melting temperature of poly(chlorotrifluoroethylene). *J. Res. Natl. Bur. Stand.* **66A,** 13–28 (1962).

16 Marand, H., Xu, J. & Srinivas, S. Determination of the equilibrium melting temperature of polymer crystals: linear and nonlinear hoffman-weeks extrapolations. *Macromolecules* **31,** 8219–8229 (1998).

17 Xu, J., Srinivas, S., Marand, H. & Agarwal, P. Equilibrium melting temperature and undercooling dependence of the spherulitic growth rate of isotactic polypropylene. *Macromolecules* **31,** 8230–8242 (1998).

18 Wu, P. L. & Woo, E. M. Linear versus nonlinear determinations of equilibrium melting temperatures of poly(trimethylene terephthalate) and miscible blend with

poly(ether imide) exhibiting multiple melting peaks. *J. Polym. Sci. Part B Polym. Phys.* **40,** 1571–1581 (2002).

19 Al-Hussein, M. & Strobl, G. The melting line, the crystallization line, and the equilibrium melting temperature of isotactic polystyrene. *Macromolecules* **35,** 1672–1676 (2002).

20 Finelli, L., Lotti, N., Munari, A., Gazzano, M. & Malta, V. Poly(thiodiethylene adipate): melting behavior, crystallization kinetics, morphology, and crystal structure. *J. Polym. Sci. Part B Polym. Phys.* **42,** 553–566 (2004).

21 Fichera, A. M., Finelli, L., Gazzano, M., Lotti, N. & Munari, A. Multiple melting behaviour of poly(thiodiethylene terephthalate): further investigations by means of X-ray and thermal techniques. *Macromol. Chem. Phys.* **205,** 63–72 (2004).

22 Flory, P. J. Theory of crystallization in copolymers. *Trans. Faraday Soc.* **51,** 848–857 (1955).

23 Baur, H. & Baltorowicz, M. Influence of sequence-length. Distribution on the melting end point of copolymers. *Makromol. Chem.* **98,** 297–301 (1966).

24 Sanchez, I. C. & Eby, R. K. Thermodynamics and crystallization of random copolymers. *Macromolecules* **8,** 638–641 (1975).

25 Helfand, E. & Lauritzen, J. I. Theory of copolymer crystallization. *Macromolecules* **6,** 631–638 (1973).

26 Gazzano, M., Soccio, M., Lotti, N., Finelli, L. & Munari, A. *J. Therm. Anal. Cal.* (submitted for publication).

27 Avrami, M. J. Granulation, phase change and microstructure. Kinetics of phase change III. *J. Chem. Phys. Chem. Phys.* **9,** 177–184 (1941).